polymer at high purity, therefore, it is essential that the molecular weight distributions of the components in a polymerization product are so sharp that their purities after fractionation can well be confirmed by sedimentation.

Acknowledgment. The authors wish to thank Professor R. Asami of Nagoya Institute of Technology for his helpful advice, the late Mr. K. Emoto for his cooperation in preparation, Mr. T. Watanabe and Mr. T. Imura for their cooperation in glass blowing, and also Dr. K. Kitagawa for his help in analysis of the initiator.

References and Notes

(1) M. Morton, T. E. Helminiak, S. P. Gadkary, and F. Bueche, *J. Polym. Sci.*, **57**, 471 (1962).
(2) T. A. Orofino and F. Wenger, *J. Phys. Chem.*, **67**, 566 (1963).
(3) T. Altares, Jr., D. P. Wyman, V. R. Allen, and K. Meyersen, *J. Polym. Sci. Part A*, **3**, 4131 (1965).
(4) S. P. S. Yen, *Makromol. Chem.*, **81**, 152 (1965).
(5) R. P. Zelinski and C. F. Wofford, *J. Polym. Sci. Part A*, **3**, 93 (1965).
(6) J. A. Gervasi and A. B. Gosnell, *J. Polym. Sci. Part A-1*, **4**, 1391 (1966).
(7) D. J. Worsfold, J. G. Zilliox, and P. Rempp, *Can. J. Chem.*, **47**, 3379 (1969).
(8) J. C. Meunier and R. Van Leempat, *Makromol. Chem.*, **142**, 1 (1971).
(9) (a) T. Masuda, Y. Ohta and Y. Onogi, *Polym. Prepr., Am. Chem. Soc., Div. Polym. Chem.*, **12 (1)**, 346 (1971); (b) T. Masuda, Y. Ohta, and S. Onogi, *Macromolecules*, **4**, 763 (1971).
(10) J. Herz and C. Strazielle, *C. R. Hebd. Seances Acad. Sci., Ser. C*, **272**, 747 (1971).
(11) J. E. L. Roovers and S. Bywater, *Macromolecules*, **5**, 384 (1972).
(12) J. E. L. Roovers and S. Bywater, *Macromolecules*, **7**, 443 (1974).
(13) M. Szwarc "Carbanions, Living Polymer and Electron Transfer Processes", Interscience, New York, N.Y., 1968.
(14) R. Asami et al., Presented at the 18th Symposium on Macromolecules, Japan 1969.
(15) T. Fujimoto, N. Ozaki, and M. Nagasawa, *J. Polym. Sci., Part A*, **3**, 2259 (1965).
(16) B. Ziegler and M. Schenell, *Justus Liebigs Ann. Chem.*, **437**, 255 (1924).
(17) W. H. Stockmayer and M. Fixman, *Ann. N.Y. Acad. Sci.*, **57**, 334 (1953).
(18) M. Kurata and M. Fukatsu, *J. Chem. Phys.*, **41**, 2934 (1964).
(19) J. G. Kirkwood, *J. Polym. Sci.*, **12**, 1 (1953).
(20) K. Mizutani, Master's thesis in Nagoya University, 1970.
(21) H. Fujita, "Foundations of Ultra-Centrifugal Analysis", Wiley, New York, N.Y., 1975.
(22) T. Kato, K. Miyaso, I. Noda, T. Fujimoto, and M. Nagasawa, *Macromolecules*, **3**, 777 (1970); I. Noda, K. Mizutani, T. Kato, T. Fijimoto, and M. Nagasawa, *ibid.*, **3**, 787 (1970).
(23) H. G. Elias, *Makromol. Chem.*, **24**, 30 (1959).
(24) Y. Kato, T. Hashimoto, T. Fujimoto, and M. Nagasawa, *J. Polym. Sci.*, **13**, 1849 (1975).

Instantaneous Shape and Segmental Density of Flexible Linear Macromolecules. 3. Partly Iodized Polystyrene in Untagged Polystyrene

Shaul M. Aharoni

Chemical Research Center, Allied Chemical Corporation, Morristown, New Jersey 07960.
Received February 17, 1978

ABSTRACT: In this work it is shown that when individual partly iodized polystyrene (IPS) molecules are suspended as a solid solution in a polystyrene (PS) matrix they are irregular in shape and possess a gross segmental density intermediate between uniform and Gaussian upon which fluctuations of the order of 100–200 Å in size are superimposed. At the same time they maintain their unperturbed radius of gyration. When the IPS molecules separate from the PS matrix, individually or as aggregates, they collapse in size while their density increases.

In the two previous papers of this series we have demonstrated that when no phase separation takes place, individual macromolecules of tagged poly-*cis*-isoprene (PIP) in untagged PIP[1] and tagged PIP in a polyisobutylene (PIB) matrix[2] possess neither spherical symmetry nor symmetrical or monotonically increasing segmental distribution density upon progressing from the molecular perimeter to its center. In both instances the instantaneous shape of the tagged PIP molecules was irregular. Internally, the segmental distribution appears as an association of high-density regions intermixed with regions of lower segmental density. The high-density regions tend, on the average, to be closer to the geometrical center of the macromolecule. Oftentimes an apron of low-density material extends out at the molecular periphery. It is obvious that when averaged over all angles and/or a large population of observable molecules, the shape and segmental density of the molecules become spherical and Gaussian.

In this work we use partly iodized polystyrene (IPS) molecules suspended in polystyrene (PS) matrix to determine whether the characteristics observed previously in PIP show also in other polymers.

Experimental Section

All solvents were reagent grade or better. They were distilled and kept over molecular sieves. Bromoform was kept in the dark. Polystyrene (PS) of $M = 2 \times 10^6$ and $M_w/M_n \leq 1.3$ was obtained from Pressure Chemical Co. (Lot 14b). Partial iodination of PS, exclusively in the para position, was performed according to the procedure of Braun.[3] For this work, the PS was iodized to the extent of 27 wt % (about half the rings are substituted) and used as such. In all preparations only PS of $M = 2 \times 10^6$ and the partly iodized PS (IPS) originating from such PS were used.

Samples for electron microscopy were prepared in the following manner: Mixtures containing 0.5, 1, 5, and 10% by weight of IPS in PS were dissolved in chloroform to yield 1% (wt/vol) solutions. The homogeneous solutions were cast in shallow Teflon-coated trays and the solvent was removed as fast as possible in forced air draft. Solid films, not completely dried but easily handlable, were obtained within several seconds. Once dried under vacuum, their thickness ranged usually between 0.3 and 0.6 mm. The samples were then prepared for examination with a transmission electron microscope using a Reichert OMU3-FC2 microtome. They were first embedded in Maraglas (Ladd Research Ind., Inc.) epoxy embedding medium which was hardened by curing at 50 °C overnight. The embedded samples were sectioned at room temperature using water as a receiving medium. Ultrathin sections of 500 to 900 Å in thickness were obtained. The sections were each mounted on a 200-mesh nickel grid. They were examined with a Hitachi HU-11C transmission electron microscope at 75 kV using a low beam current at magnifications of 24 000 and 52 000 times. Several grids were prepared from each sample, and several photographs were taken from each grid. The photographs presented in this paper are true representatives of the corresponding samples.

The unperturbed radius of gyration R_{GO} of the tagged IPS, as calculated[4] from the $M = 2 \times 10^6$ of the parent PS, is 390 Å; in a good

0024-9297/78/2211-0677$01.00/0

solvent R_G is, naturally, larger than R_{GO}. The actual diameter of the corresponding molecule is about the thickness of the ultrathin microtomed sections, resulting in whole and parts of tagged molecules being observed in the sections. When the molecules are completely random and do not possess any shape or segmental distribution symmetry, then the exact shape of the parts of the tagged molecules remaining in the microtomed section is unimportant. Observation of many such parts of molecules will still yield the desired information concerning the instantaneous shape and segmental distribution of the intact molecules. On the other hand, if the molecules do have a shape and segmental distribution symmetry, then the knowledge of the shape of the observed part is of cardinal importance in the determination of the segmental density in the parent molecule. A discussion of this point was presented in paper 2 of this series.[2]

To study the density distribution in the photographed particles, scans across many of their images on the glass electron image plates were performed with the aid of a Joyce, Loebl and Co. Ltd., double-beam recording microdensitometer MK III CS, operating in the 0–3 range of optical density to insure linearity in the transfer of the intensity from the electron image plate to the densitometer chart. The shape of the scanned area at each instant was an oblong 0.9 × 0.3 mm in size. This window was moving on the electron image plate in one direction, leaving behind a scanned path 0.9 mm wide. Since the microdensitometer averages the optical density in the instantaneously scanned window, fine details that were observed in the printed photographs were oftentimes smeared out. The densitometer scans were performed only on regions that were neither underexposed nor overexposed, to eliminate artifacts due to nonlinearity in the response of the electron image plates, or excessive scattering, as the case may be. The relation between the electron density in particles in the sample and the optical density of their images on the electron image plates is considered to be linear[5] in the intermediate density range used for the densitometer scans.

Depending on the magnification in the electron microscope, the size of the densitometer window corresponds to 120 down to 60 Å. Because of these small sizes it was found that the window opening did not noticeably affect the observations and conclusions arising from the microdensitometer scans.

Results and Discussion

As was described in the Experimental Section, several solid samples of varying concentrations of IPS in PS were prepared for the purpose of studying them by means of the electron microscope. When observed under high magnification in the transmission mode, all the samples exhibit two characteristic features: (1) Regions where there exists a gradual change in local concentration, from a few individual molecules of IPS scattered in a matrix of PS, through carpets of individual IPS molecules seen on a background of PS (Figure 1), through areas of apparent equal concentrations of IPS and PS (Figure 2), to areas where a few PS molecules are seen embedded in an electron-dense IPS matrix (Figure 3). These regions of change in concentration span the areas between zones of apparently pure PS and apparently uniform IPS, which were also seen in the samples. (2) Regions where individual IPS molecules tended to become spherical in shape while others tended to aggregate in spherical aggregates each containing many IPS molecules (Figures 4 and 5). The above two characteristics appear not to coexist in the same field of vision.

The overall concentration dependence of areas exhibiting the first characteristic was manifested by an increase in the frequency of IPS-rich zones with the increase in overall concentration of IPS in PS. In areas exhibiting the second characteristic, the concentration dependence was manifested by an increase in the number and size of the IPS polymolecular spherical aggregates as a function of concentration.

The gross appearance of the IPS-rich zones seems to be independent of the overall IPS concentration. At their outskirts only a few electron-dense entities scattered in an electron-dilute PS matrix are observed. Upon progression toward the more IPS concentrated regions the number of such entities increases, oftentimes passing through carpets of such entities embedded in PS as is shown in the typical Figure 1. At higher IPS local concentrations we pass through regions of apparent

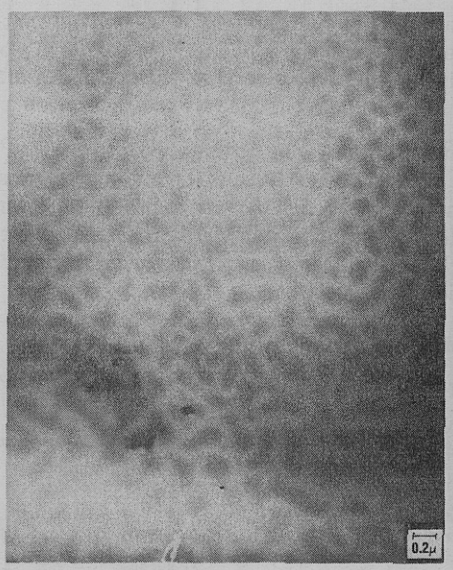

Figure 1. A carpet of IPS molecules dissolved in PS matrix. Overall concentration 1% IPS in PS.

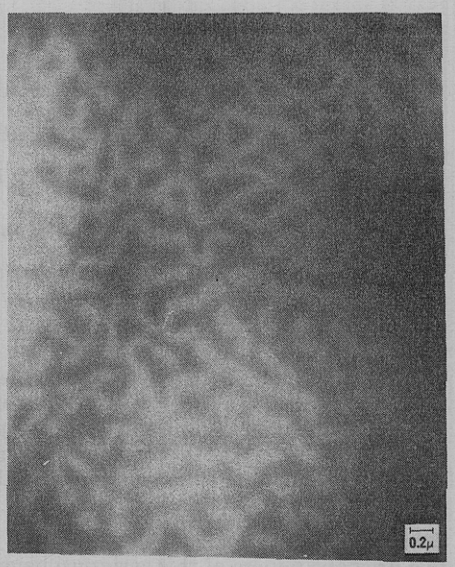

Figure 2. An area of apparent equal concentrations of IPS and PS molecules. In reality, necklaces of IPS molecules dissolved in PS matrix. Overall concentration 1% IPS in PS.

half and half IPS and PS, as seen in Figure 2, where the IPS and PS appear to phase separate in a spinodal manner. At even higher IPS concentration, regions as are shown in Figure 3 become common, revealing individual electron-dilute entities existing in an electron-dense matrix of IPS.

Figures typical of areas exhibiting the second characteristic above are Figure 4 and under much higher magnification Figure 5. Note that the smaller high-density entities, which we believe to be images of individual IPS molecules, are significantly smaller than those in Figures 1 and 3. Also, note that the density of the smaller particles in Figures 4 and 5 is significantly higher than that of the individual particles in Figures 1 and 3. It may be that the large entities were disrupted by the sectioning procedure to reveal their internal structure.

The electron-dense images in Figure 1 are devoid of circular symmetry. This indicates that the imaged particles, in the sample itself, lack spherical symmetry. Measurements of many such particles yielded an average diameter of 1000 Å.

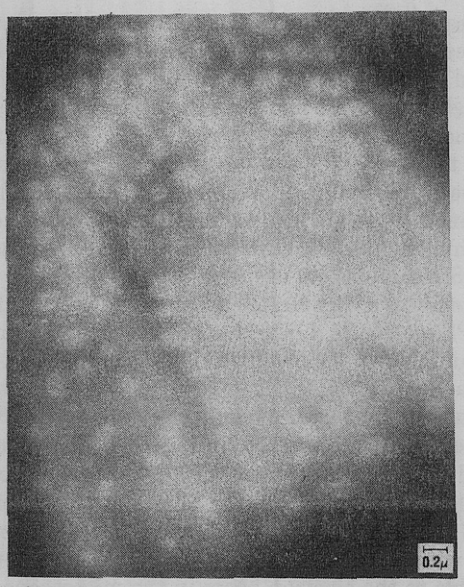

Figure 3. An area of apparently higher concentration of IPS than PS. In reality a solution of IPS in PS in which areas occasionally unoccupied by ISP molecules appear as electronically dilute voids in electronically dense matrix.

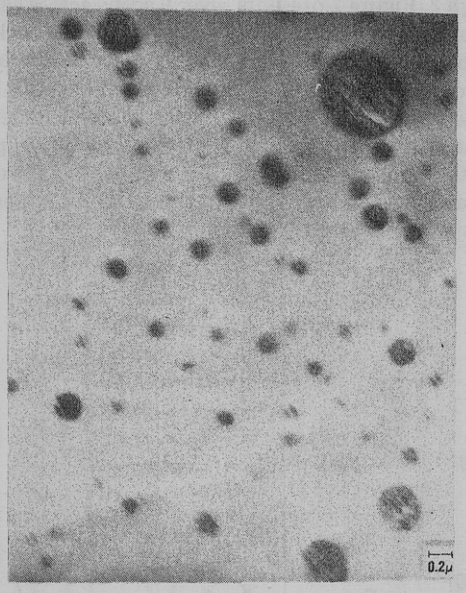

Figure 4. Phase-separated area. Note the striations in the multimolecular dense aggregates, delineating individual IPS molecules.

In Figure 3 one observes the reverse case, of individual electron-dilute entities embedded in electron-dense matrix. These entities, similar to those seen in Figure 1, lack spherical symmetry. Their size is about 1000 Å, similar to the size of the individual electron-dense entities in Figure 1.

The unperturbed radius of gyration, R_{GO}, of the parent PS molecules of $M = 2 \times 10^6$ is about 390 Å, yielding an unperturbed diameter of the equivalent sphere[6] of $(5/3)^{1/2} \times 390 \times 2 = 1010$ Å. The agreement between the sizes of the individual electron-dense and electron-dilute entities (Figures 1 and 3) on one hand and the expected size of the PS macromolecules in the amorphous glass is excellent. It is obvious that, at least in the case of PS, the observed 1000 Å size individual electron-dilute particles are individual PS macromolecules of $M = 2 \times 10^6$. We note that the characteristic ratios of poly(*p*-chlorostyrene) and poly(*p*-bromostyrene) are 10.6 ± 0.6 and 12.3 ± 1.1,[7–13] respectively, as compared with 10 ± 0.2 for PS.[14]

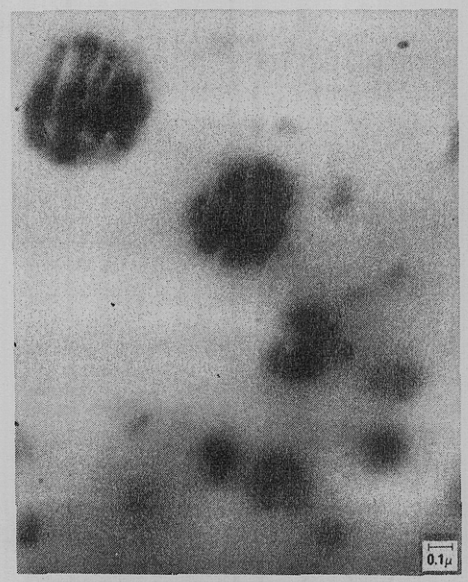

Figure 5. Phase-separated area under magnification much higher than in Figure 4. Note the subdivision of the multimolecular dense aggregates into individual IPS molecules.

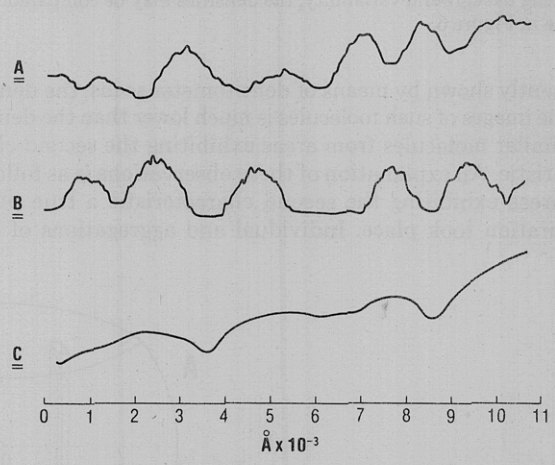

Figure 6. Microdensitometer scans across areas of varying local concentration of IPS in PS. Scan A: typical of areas such as shown in Figure 1. Scan B: typical of areas such as shown in Figure 2. Scan C: typical of areas such as shown in Figure 3.

This indicates that the R_{GO} of the para-halogenated PS is not dramatically larger than that of pure PS. Recalling that our IPS is only partly iodized and the parent PS is also of $M = 2 \times 10^6$, one expects its R_{GO} to be reasonably close to that of the parent PS. Even when the IPS molecules are suspended in PS matrix their R_G is not expected to increase significantly above R_{GO}, because they are only partly substituted with iodine. The fact that R_G of partly iodized PS even up to 50% by weight iodine does not increase much above R_{GO} when the IPS is suspended in PS was demonstrated by Hayashi et al.[15,16] in their small-angle X-ray scattering (SAXS) studies on such samples. From the discussion above, it becomes obvious that the individual electron-dense particles of about 1000 Å in diameter, visible in the typical Figure 1, are individual IPS macromolecules. Naturally, their complete absence in blank samples comprised of pure PS and the embedding epoxy material was repeatedly verified.

The observed sizes of individual IPS molecules in Figure 1, and PS molecules in Figure 3, correspond very well with their R_{GO}'s. As is easily seen from the figures and as will be

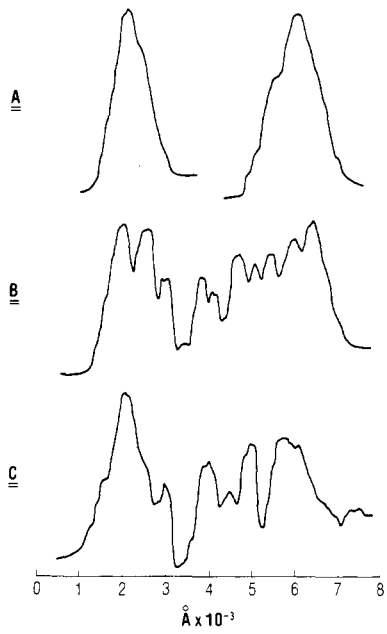

Figure 7. Microdensitometer scans across areas typified by Figure 4. Scan A: two small aggregates of IPS molecules. Scans B and C: two such large aggregates. Internal structure is clearly noticeable. Neglecting background variability, the densities may be compared with those in Figure 6.

presently shown by means of densitometer scans, the density of the images of such molecules is much lower than the density of similar molecules from areas exhibiting the second characteristic. An explanation of these observations is as follows: In areas exhibiting the second characteristic a true phase separation took place. Individual and aggregations of IPS molecules separated out of the PS matrix. The individual molecules are collapsed on themselves in order to fill their pervaded volume with IPS segments. The collapsed molecules are of high density. To minimize their interfacial energy with the PS matrix, they tend to sphericity. If not interrupted, they proceed to form larger and larger spherical aggregates. Because these are comprised of collapsed IPS molecules, their microtomed slices are also very dense. On the other hand, areas exhibiting the first characteristic are true solid solutions. Here IPS molecules are suspended in a PS matrix with PS segments filling a very large fraction of the pervaded volume of the IPS molecules. Local changes in concentration of IPS are accountable for the observed changes in Figures 1 through 3, from a few IPS molecules in a PS field through carpets of IPS molecules (in Figure 1), and areas where the IPS molecules become interconnected (in Figure 2), to regions where the solid solution is almost uniform except for an occasional IPS molecule missing from the observed thin microtomed section (in Figure 3). Areas where the IPS concentration was high, as within the large entities in Figures 4 and 5, were impenetrable to the electron beam in the microscope and appeared as intensely dark areas in the developed photomicrographs.

Microdensitometer scans across the images of individual macromolecules on the electron image plates are shown in Figures 6 and 7. Figure 6 is typical of areas such as in Figures 1 through 3. Figure 7 presents several scans across aggregates typical of Figures 4 and 5. The gentle slant of the background, noticeable in almost all the scans, is most probably due to gradual changes in the overall thickness of the sample sections. Since the scans in Figures 6 and 7 were obtained, under exactly the same instrument setting, from electron image plates of exactly the same magnification, a comparison of the densities of the particles and aggregates in these figures appears to be valid. It will be presently discussed.

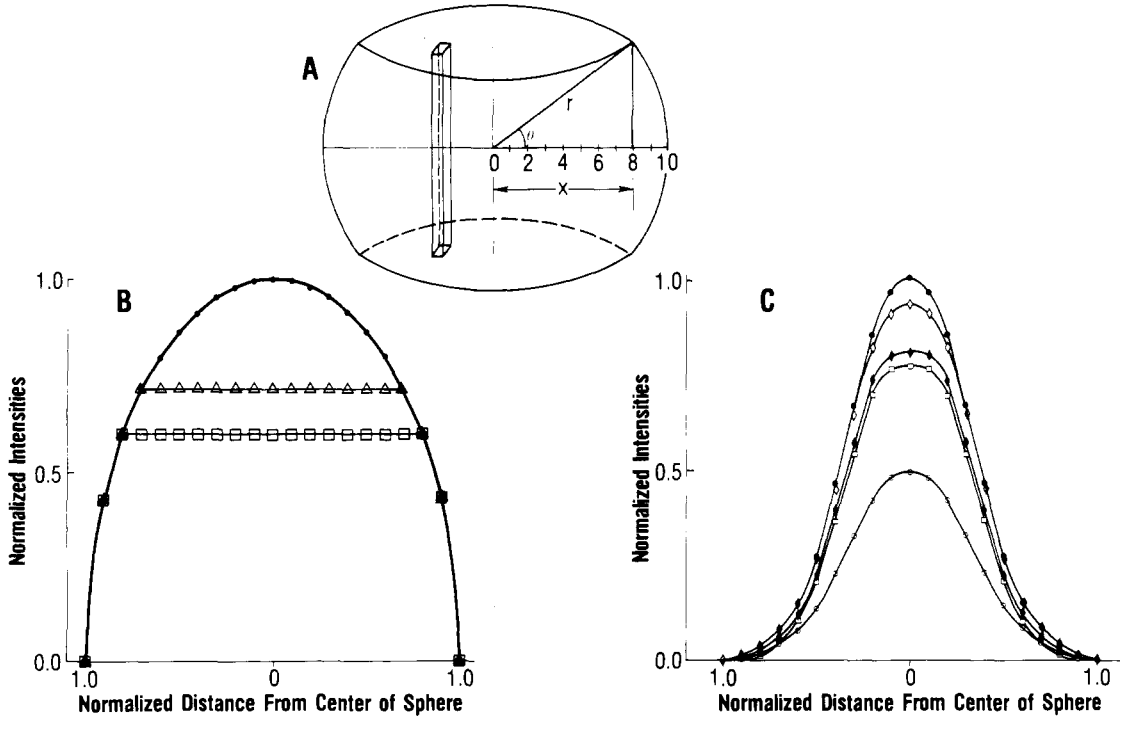

Figure 8. (A) Definition of the ratio x/r, determining the height of a barrel obtained by sectioning a sphere, x is the projection of r on a plane perpendicular to the direction of the electron beam through the imaged entity. The oblong prism represents the volume corresponding to the oblong shape instantaneously scanned on the image plate by the microdensitometer. (B) Integrated densities for a sphere and its parts under a uniform density assumption: (●) sphere, (□) barrel with $x/r = 0.8$, (△) barrel with $x/r = 0.7$. (C) Integrated densities for a sphere and its parts under the assumption of a Gaussian density: (●) sphere, (○) hemisphere, (□) barrel with $x/r = 0.9$, (♦) barrel with $x/r = 0.8$, (◇) barrel with $x/r = 0.6$.

For the purpose of obtaining a qualitative estimate of the shape of the segmental density within the individual IPS molecules, one resorts to several simple procedures described in detail in paper 2 of this series.[2] One approach is to notice that the imaged densities are two-dimensional projections of the actual densities and that images of fragments of spherical particles (or particles tending to sphericity) do not yield the same density distribution as images of intact particles. The densities of whole spheres, hemispheres, and several additional fragments, calculated on the basis of either uniform segmental density or Gaussian segmental density within the observed particle, are presented in Figure 8. Another approach utilizes the fact that the shape of the segmental distribution curve at the peripheral parts of the imaged particle is very strongly dependent on the segmental distribution in the actual part. The curve arising from uniform density is distinctly convex while the curve arising from Gaussian distribution is distinctly concave; a comparison of the actual scans with the calculated expectations is most revealing and easy to perform.

A glance at Figure 6, traces A and B, reveals that the segmental density within the observed particles, all of about 1000 Å in size, is intermediate between a uniform distribution and a Gaussian one. The electron-dilute particles in trace C of the figure seem to have an inverted Gaussian density but this appears to be caused by the peripheral zones of particles, with intermediate segmental distribution, coalescing to form an electron-dense boundary around an electron-dilute cavity.

During the process of phase separation the tendency toward molecular collapse becomes very evident: the IPS molecules decrease in size and exclude more and more PS segments from their pervaded volume. This is reflected in the electron image plate, and in the microdensitometer scans, by the diameter of the imaged molecule becoming much smaller than in the solid solution, by the electron density within the particles image becoming much higher, and by the tendency toward a uniform segmental density within such particles. Phase-separated aggregates of the IPS molecules oftentimes showed their internal structure (cf. Figures 4, 5, and 7) and the densitometer scans reveal the uniformity of the segmental density, and the high electron density, of each IPS molecule within the aggregate (Figure 7, traces B and C). At the perimeter of the aggregate some dilution of IPS by PS takes place, leading to a gradual change in segmental density. The sharp slope of the corresponding scans (Figure 7, traces A, B, and C) and the distribution of mass within the particle (Figure 7, trace A), that does not follow the distribution under the bell-shaped Gaussian curve, indicate that the IPS segmental distribution within the aggregates and at their perimeters is not Gaussian but of higher density.

While being non-Gaussian, the segmental density of the IPS molecules, as scanned in Figure 6, increases upon progressing from the perimeter of each molecule to its center. The density distribution is not monotonic, however, showing many small fluctuations whose size is of the order of 100–200 Å. These density fluctuations are not as large and each involves smaller size than those previously observed in tagged PIP,[1,2] but they are undoubtedly real. This is corroborated by the fact that densitometer scans of background areas of such Figures as 1, 2, 4, or 5, and aggregates as are shown in Figure 7, show much smaller fluctuations (less than 50 Å in size), if at all, than those observed in the scans of IPS molecules (Figure 6, scans A and B) and aggregates (Figure 6, scan C). These smaller fluctuations most probably arise from the fine grain of the electron image plates and instrumental noise in the microdensitometer.

Finally, a word about the noncircular shape of the macromolecules. As was stressed in the first paper of this series,[1] the molecules one observes have an irregular shape of the perimeter and, prior to averaging, their segmental density is not describable by a smooth, monotonic or bell-shaped distribution. Theoretical models originating from random flight calculations,[17–40] even those assuming instantaneous asphericity,[24–26,28–40] possess a segmental distribution smoothly and monotonically increasing from the periphery toward a single maximum at the center of the macromolecule, or thereabouts. In agreement with these averaged models, when the observed segmental distribution was averaged over many molecules, in the second paper of this series,[2] the averaged segmental distribution turned out indeed to be Gaussian. Rotation of the observed macromolecules over all angles yields a spherically symmetrical shape. If one merely smooths the shape irregularities of the instantaneously observed molecules, then one finds that the ratios of the radii of the resultant ellipsoids (the two-dimensional projections of the actual molecules) are about 1.3–1.5:1.0. We have never observed a ratio of radii exceeding 2:1. A more detailed study of these aspects must wait acquisition of additional data.

References and Notes

(1) S. M. Aharoni, *Polymer*, **19**, 401 (1978).
(2) S. M. Aharoni, *J. Macromol. Sci., Phys.*, in press.
(3) D. Braun, *Makromol. Chem.*, **30**, 85 (1959).
(4) M. Kurata, Y. Tsunashima, M. Iwama, and K. Kamada, in "Polymer Handbook", 2nd ed, J. Brandrup and E. H. Immergut, Ed. Wiley, New York, N.Y., 1975, p IV-1 ff.
(5) Anon, "Kodak Electron Image Plates", Kodak Pamphlet No. P-116, Eastman Kodak Co. Rochester, N.Y..
(6) C. Wolff, *Eur. Polym. J.*, **13**, 739 (1977).
(7) J. E. Davis, Ph.D. Thesis, MIT, Cambridge, Mass. 1960.
(8) N. Kuwahara, K. Ogino, A. Kasai, S. Ueno, and M. Kaneko, *J. Polym. Sci., Part A*, **3**, 985 (1965).
(9) I. A. Baranovskaya and V. Ye. Eskin, *Polym. Sci. USSR (Engl. Transl.)*, **7**, 373 (1965).
(10) R. B. Mohite, S. Gundiah, and S. L. Kapur, *Makromol. Chem.*, **116**, 280 (1968).
(11) Y. Noguchi, A. Aoki, G. Tanaka, and H. Yamakawa, *J. Chem. Phys.*, **52**, 2651 (1970).
(12) K. Takashima, G. Tanaka, and H. Yamakawa, *Polym. J.*, **2**, 245 (1971).
(13) J. E. Mark, *J. Chem. Phys.*, **56**, 458 (1972).
(14) P. J. Flory, "Statistical Mechanics of Chain Molecules", Interscience, New York, N.Y., p 40.
(15) H. Hayashi, F. Hamada, and A. Nakajima, *Macromolecules*, **9**, 543 (1976).
(16) H. Hayashi, F. Hamada, and A. Nakajima, *Makromol. Chem.*, **178**, 827 (1977).
(17) P. J. Flory, "Principles of Polymer Chemistry", Cornell University Press, Ithaca, N.Y., 1953, p 399 ff.
(18) C. Tanford, "Physical Chemistry of Macromolecules", Wiley, New York, N.Y., 1961, p 138 ff.
(19) H. Tompa, "Polymer Solutions", Butterworths, London, 1956, p 233 ff.
(20) W. H. Stockmayer, *Makromol. Chem.*, **35**, 54 (1960).
(21) P. Debye and F. Bueche, *J. Chem. Phys.*, **20**, 1337 (1952).
(22) P. J. Flory and S. Fisk, *J. Chem. Phys.*, **44**, 2243 (1966).
(23) W. R. Krigbaum and P. J. Flory, *J. Chem. Phys.*, **20**, 873 (1952).
(24) J. Mazur and D. McIntyre, *Macromolecules*, **8**, 464 (1975).
(25) K. Solc and W. H. Stockmayer, *J. Chem. Phys.*, **54**, 2756 (1971).
(26) P. H. Lindenmeyer, *J. Appl. Phys.*, **46**, 4235 (1975).
(27) W. Kuhn, *Kolloid-Z.*, **68**, 2 (1934).
(28) W. C. Forsman and R. E. Hughes, *J. Chem. Phys.*, **38**, 2118 (1963).
(29) W. C. Forsman and R. E. Hughes, *J. Chem. Phys.*, **38**, 2123 (1963).
(30) K. Solc, *J. Chem. Phys.*, **55**, 335 (1971).
(31) W. Gobush, K. Solc, and W. H. Stockmayer, *J. Chem. Phys.*, **60**, 12 (1974).
(32) J. Bendler, K. Solc, and W. Gubush, *Macromolecules*, **10**, 635 (1977).
(33) F. L. McCrackin, J. Mazur, and C. M. Guttman, *Macromolecules*, **6**, 859 (1973).
(34) J. Mazur, C. M. Guttman, and F. L. McCracklin, *Macromolecules*, **6**, 872 (1973).
(35) P. H. Verdier and W. H. Stockmayer, *J. Chem. Phys.*, **36**, 227 (1962).
(36) D. E. Kranbuehl and P. H. Verdier, *J. Chem. Phys.*, **56**, 3145 (1972).
(37) D. E. Kranbuehl, P. H. Verdier, and J. M. Spencer, *J. Chem. Phys.*, **59**, 3861 (1973).
(38) P. H. Verdier, *J. Chem. Phys.*, **59**, 6119 (1973).
(39) D. E. Kranbuehl and P. H. Verdier, *J. Chem. Phys.*, **67**, 361 (1977).
(40) B. E. Eichinger, *Macromolecules*, **10**, 671 (1977).